

Spectral analysis of femtosecond pulse diffraction through binary diffractive optical elements: theory and experiment

Omel Mendoza-Yero, Gladys Mínguez-Vega, Jesús Lancis, Enrique Tajahuerce, and Vicent Climent

*GROC, Departament de Física, Universitat Jaume I, E12080 Castelló, Spain
omendoza@uji.es*

Abstract: We report on the changes in the spectrum of a femtosecond pulse originated by diffraction of the ultrashort waveform through a circularly symmetric binary diffractive optical element. The analysis is performed in the framework of the Rayleigh-Sommerfeld formulation of the diffraction, where an analytical expression for the monochromatic amplitude distribution close to the optical axis is obtained. To corroborate our results, we experimentally measure the variations of the pulse spectrum within the collecting area of a spectrometer located at the output plane. Multiple splitting of the pulse spectrum in the vicinity of a focal position and a phase singularity are shown.

©2008 Optical Society of America

OCIS codes: (070.4790) Spectrum analysis; (120.6200) Spectrometers and spectroscopic instrumentation; (260.1960) Diffraction theory; (320.2250) Femtosecond phenomena.

References and links

1. G. Gbur, T. D. Visser, and E. Wolf, "Anomalous Behavior of Spectra near Phase Singularities of Focused Waves," *Phys. Rev. Lett.* **88**, 013901 (2002).
2. G. Popescu and A. Dogariu, "Spectral Anomalies at the Wave-Front dislocations," *Phys. Rev. Lett.* **88**, 183902 (2002).
3. S. A. Ponomarenko and E. Wolf, "Spectral anomalies in a Fraunhofer diffraction pattern," *Opt. Lett.* **27**, 1211-1213 (2002).
4. D. Ganic, J. W. M. Chon, and M. Gu, "Effect of numerical aperture on the spectral splitting feature near phase singularities of focused waves," *Appl. Phys. Lett.* **82**, 1527-1528 (2003).
5. L. E. Helseth, "Spectral density of polychromatic electromagnetic waves," *Phys. Rev. E* **73**, 026602 (2006).
6. Z. Liu and B. Lü, "Spectral shifts and spectral switches in diffraction of ultrashort pulsed beams passing through a circular aperture," *Optik* **115**, 447-454 (2004).
7. S. P. Veetil, N. K. Viswanathan, C. Vijayan, and F. Wyrowski "Spectral and temporal evolutions of ultrashort pulses diffracted through a slit near phase singularities," *Appl. Phys. Lett.* **89**, 041119 (2006).
8. S. Jana and S. Konar, "Tunable spectral switching in the far field with a chirped cosh-Gaussian pulse," *Opt. Commun.* **267**, 24-31 (2006).
9. Q. Cao and J. Jahns, "Modified Fresnel zone plates that produce sharp Gaussian focal spots," *J. Opt. Soc. Am. A* **20**, 1576-1581 (2003).
10. O. Mendoza-Yero, G. Mínguez-Vega, J. Lancis, M. Fernández-Alonso, and V. Climent, "On-axis diffraction of an ultrashort light pulse by circularly symmetrical hard apertures," *Opt. Express.* **15**, 4546-4556 (2007).
11. O. Mendoza-Yero, G. Mínguez-Vega, J. Lancis, and V. Climent, "Focusing and spectral characteristics of periodic diffractive optical elements with circular symmetry under femtosecond pulsed illumination," *J. Opt. Soc. Am. A* **24**, 3600-3605 (2007).
12. S. D. Feller, H. Chen, D. J. Brady, M. E. Gehm, C. Hsieh, O. Momtahan, and A. Alibi, "Multiple order coded aperture spectrometer," *Opt. Express.* **15**, 5625-5630 (2007).

1. Introduction

Spectral behavior of focused waves having a broad spectrum has been a matter of increasing scientific attention during the past few years. In particular, a strong dependence of the on-axis

spectrum on the axial position for polychromatic spatially coherent light focused by a hard aperture has been demonstrated. This kind of illumination corresponds, for instance, to that emitted by a femtosecond laser source. Also, a collimated thermal source could be employed. Although several experiments to corroborate diffraction-induced spectral modifications can be thought, in general, they are difficult to implement because of the still high cost of femtosecond sources and/or the sometimes low signal-to-noise ratio presented at the measuring point. This last situation is particularly relevant in the case of a phase singularity, a point where the intensity of the diffracted field has a zero value. At such points, the phase becomes indeterminate and the field in the neighborhood has a complex structure exhibiting dislocation and vortices.

Dramatic spectral changes near the focus of a converging spatially coherent polychromatic field diffracted by a hard aperture were predicted by Gbur et al. [1]. Among them, the two-lobe splitting of the initial spectrum and the gradual change of the spectral shift, the so-called spectral switch, were experimentally verified [2]. Spectral anomalies associated with broadband fields in the vicinity of the dark rings of the Airy pattern have been theoretically predicted [3]. In this aspect, both the effect of the numerical aperture of the system [4] and the vectorial nature of the electromagnetic field have been taken into account [5]. Within the scalar approximation and the paraxial regime, some analytical expressions for the on-axis power spectrum of an ultrashort pulse diffracted through a circular aperture have been derived [6]. Furthermore, in recent years, spectral and temporal evolutions of a Gaussian pulse diffracted through a slit, near phase singularities, were investigated by means of a numerical simulation technique [7]. The possibility of tunable spectral switching and spectral shifts was also elucidated [8].

In this letter, we provide an approximate analytical expression beyond the paraxial approximation for the off-axis wave field generated by the diffraction of a monochromatic plane wave through a circularly symmetric binary diffractive optical element (DOE). This expression, determined within the framework of the Rayleigh-Sommerfeld diffraction theory, allows us to compute the spectral behavior of the wave field under broadband illumination both for the on-axis and the off-axis cases. To test the validity of our formulation, the changes in the spectrum of a 10 femtosecond ultrashort pulse diffracted through a binary DOE are discussed. In particular, the power spectrum of the diffracted pulse at a focal position of the DOE is experimentally measured. By taking into account the dispersion of the wave field at the collecting area of the spectrometer, we show that the measured data are in well agreement with our formulation. On the other hand, the spectrum splitting at the first phase singularity associated with the central frequency of the pulse is numerically simulated.

2. Basic theory

Let us consider a circularly symmetric binary DOE consisting of N transparent rings, with N an integer positive number. The polar coordinates r, θ are assumed at the input plane, whereas for any parallel output plane, located at a distance z from the DOE, corresponding coordinates R, φ are used, see Fig. 1.

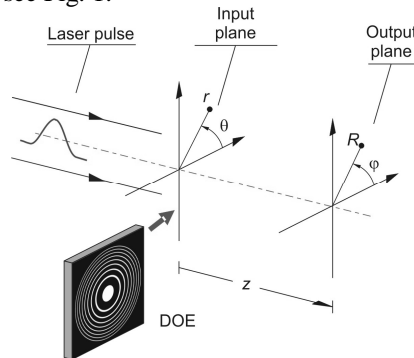


Fig. 1. Definition of the diffraction (input) plane and the observation (output) plane.

The field $U_m(z, R)$ diffracted under monochromatic plane wave illumination from an annular aperture of the DOE, identified by the subscript m , can be determined through the first Rayleigh-Sommerfeld diffraction integral in the form,

$$U_m(z, R) = -\frac{z}{2\pi} \int_0^{2\pi} \int_{r_{im}}^{r_{om}} \frac{\left(ik - \frac{1}{\rho(r, \theta)} \right) \exp[ik\rho(r, \theta)]}{\rho(r, \theta)^2} r dr d\theta. \quad (1)$$

In the above formula $\rho(r, \theta) = \sqrt{z^2 + r^2 + R^2 - 2rR \cos(\theta - \varphi)}$, r_{im} and r_{om} are the inner and the outer radii of the m -th annular aperture, respectively, and k holds for the wave number; i.e., $k = 2\pi/\lambda$, with λ the wavelength. In general, it is difficult to assess an analytical expression for $U_m(z, R)$. However, an approximate result in the neighborhood of the propagation axis can be obtained. To this end, the distance $\rho(r, \theta)$ is approximated around $R=0$ by using the Taylor series expansion up to the first order to yield $\rho(r, \theta) \approx (z^2 + r^2)^{1/2} - rR \cos(\theta - \varphi)/(z^2 + r^2)^{1/2}$. Only the first term of the expansion is substituted for $\rho(r, \theta)$ in Eq. (1), except for the exponential function, where both terms are used. With the help of the identity $\int_0^{2\pi} \exp(-i\xi \cos(\theta - \varphi)) d\theta = 2\pi J_0(\xi)$, where $J_q(\xi)$ denotes the Bessel function of the first kind with q order, and after carrying out an integration by parts, we find that

$$U_m(z, R) \approx \frac{z \exp\left(ik\sqrt{z^2 + r_{im}^2} \right)}{\sqrt{z^2 + r_{im}^2}} J_0\left(\frac{kr_{im}R}{\sqrt{z^2 + r_{im}^2}} \right) - \frac{z \exp\left(ik\sqrt{z^2 + r_{om}^2} \right)}{\sqrt{z^2 + r_{om}^2}} J_0\left(\frac{kr_{om}R}{\sqrt{z^2 + r_{om}^2}} \right). \quad (2)$$

It should be pointed out that an additional contribution to the field $U_m(z, R)$ depending on the term $kRz^3 J_1(krR/(z^2 + r^2)^{1/2})$ has been neglected. The above approximation holds for points in the close vicinity of the propagation axis. Equation (2) is the main theoretical result of this paper. We note that some further approximations were used in [9] to obtain an analytical expression for the diffracted field at the main focal plane of a modified Fresnel zone plate. For the particular case of $R=0$, Eq. (2) is simplified to yield the on-axis diffracted field

$$U_m(z, 0) = \frac{z \exp\left(ik\sqrt{z^2 + r_{im}^2} \right)}{\sqrt{z^2 + r_{im}^2}} - \frac{z \exp\left(ik\sqrt{z^2 + r_{om}^2} \right)}{\sqrt{z^2 + r_{om}^2}}, \quad (3)$$

Note that Eq. (3) provides the exact on-axis solution [10]. From the superposition principle, the total diffracted field $U(z, R)$ is obtained by the sum of the contributions from each transparent ring. In mathematical terms, $U(z, R) = \sum_{m=1}^N U_m(z, R)$.

To gain further insight, we consider a periodic DOE in the squared radial coordinate, with period p^2 , and assume that each transparent ring has an identical area Σ_0 . Let us denote as $1/\varepsilon = \Sigma_0/\pi p^2$, with $\varepsilon > 1$, the opening ratio of the DOE, that is, the fraction of the transparent area within one period of the DOE. We express the inner and the outer radii as $r_{im} = p(m-1)^{1/2}$ and $r_{om} = p(m - (1-1/\varepsilon))^{1/2}$. By using Eq. (3), it can be verified [11] that the on-axis irradiance has a maximum value approximately at the axial positions $z_n = \varepsilon \Sigma_0 / (2\pi \lambda n)$, the so-called foci of the DOE, with n a positive integer. An exception occurs when the opening ratio is a rational number $\varepsilon = n/m$, with m a positive integer. In this case, the DOE focus transforms into a phase singularity where the intensity vanishes. From the above reasoning, monochromatic spectral anomalies are located at the axial positions $z_m^* = \Sigma_0 / (2\pi \lambda m)$.

3. Experimental verification

To check our approach, we experimentally measure the diffracted field in the close vicinity of an axial focal point originated by the femtosecond pulsed illumination of a DOE. From a practical point of view, spectral measurements are affected by the finite size of the light collecting area of the spectrometer. With no loss of generality we assume a fiber spectrometer. When a centered circular pinhole is placed just before the entrance of the fiber used to gather the light into the spectrometer, the integrated power spectrum, $S(\lambda)$, can be numerically evaluated by means of the expression

$$S(\lambda) = \frac{S_0(\lambda)}{A} \int_0^{2\pi r_0} \int_0^{2\pi r_0} I(z, R) R dR d\varphi. \quad (4)$$

In the above expression $S_0(\lambda)$ is the power spectrum of the incident femtosecond pulse, $I(z, R) = |U(z, R)|^2$, and $A = \pi r_0^2$ reads for the area of the pinhole with radius r_0 . From Eq. (4), it is clear that the power spectrum $S(\lambda)$ takes into account off-axis spectral contributions at points in the output plane within the area A centered around $R=0$. In this case $I(z, R)$ does not depend on φ and the signal-to-noise ratio is high. However, when considering off-axis areas far from an axial focal point, the above features are no longer true and it is becoming harder both to assess and to measure the power spectrum.

In order to validate experimentally the numerical results given by Eq. (4) for the spectrum shape, laboratory measurements were carried out. For the experiment, the DOE was manufactured by direct laser writing on a chrome photomask. The laser writing machine (Microtech, Palermo, Italy) allows us to obtain a photomask with a global resolution of 0.2 μm and a minimum feature size of 0.8 μm . The selected DOE design parameters were $\Sigma_0 = 11.78 \mu\text{m}^2$, $\varepsilon = 4$ and $N = 9$. As a broadband source, a Ti:Sapphire femtosource compact system (Femtolasers, Vienna, Austria) was employed. The laser system emits light pulses of 10 fs (full-width-at-half-maximum) at a carrier frequency of $\lambda_0 = 780 \text{ nm}$. The power spectrum of the pulsed radiation emitted from the laser is plotted in Fig. 2(c).

The selected monochromatic ($\lambda = \lambda_0$) focal position was $z_{11} = 0.87 \text{ m}$ ($n = 11$). The pulsed beam that impinges in the DOE was previously collimated. To locate the monochromatic focal point, the femtosecond laser system was running out of the mode-locked regime, where the output spectrum is nearly monochromatic. In this situation, the focal position was determined with the help of a conventional CCD camera. The output integrated power spectrum was measured with a StellarNet EPP2000 fiber optics spectrometer (wavelength range from 135 nm to 1100 nm), whose input collecting area was limited by a pinhole. Normalized numerical simulations of Eq. (4) together with corresponding experimental data, for the pinhole radii of $r_0 = 75 \mu\text{m}$ and $r_0 = 200 \mu\text{m}$, are shown in Fig. 2(a) and Fig. 2(b), respectively.

The spectrum at the vicinity of this focus is red shifted. This effect is accentuated as far as we consider diffracted pulse contributions from closer regions to the axial focus, see Fig. 2(a). In contrast, when the pinhole area is increased, the power spectrum approaches to the initial spectrum before the DOE, see Fig. 2(b) and Fig. 2(c). In general, experimental results are in well agreement with the theoretical predictions. Discrepancies are due to misalignment of the focus with respect to the pinhole position or by reduction of the spectrometer sensitivity due to the low optical power launched into the optical fiber [12]. In addition, we realized that small deviation from the plane wave behavior of the pulse gives rise to considerable variations in the position of DOE foci.

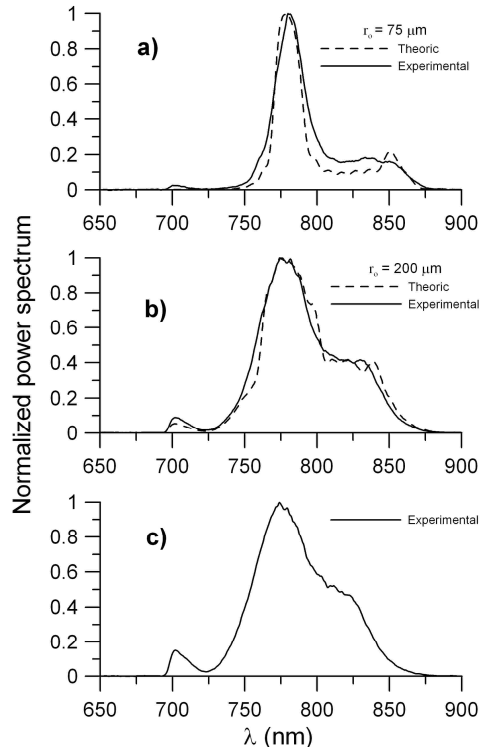


Fig. 2. Integrated output spectrum for pinholes of a) $r_0 = 75\mu\text{m}$, b) $r_0 = 200\mu\text{m}$ and c) for the incoming ultrashort pulse (without pinhole).

4. Numerical simulations

After the experimental test, Eq. (2) is also used to numerically assess the spectral changes in the vicinity of the first monochromatic spectral anomaly located at the position $z_1^* = 2.4$ m. The results are plotted in Fig. 3(a), where the output power spectrum, $I(z_1^*, R)S_0(\lambda)$, is plotted as a function of the radial coordinate R . The units for the vertical axis are arbitrary.

The output power spectrum shows an asymmetric split with several satellite peaks of variable heights. Note that the spectrum splitting is strongly dependent on the transverse coordinate. For completeness, we show in Fig. 3(b) the variation of the power spectrum, $I(z_{11}, R)S_0(\lambda)$, in the vicinity of the axial monochromatic focus point $z_{11} = 0.87$ m. After a visual inspection of Fig. 3(b) one sees that the spectrum shape remains almost unchanged for $R \leq 20\mu\text{m}$, approximately. However, for points a little more distant from the axial focus the spectrum changes quite a lot, showing for instance a further splitting.

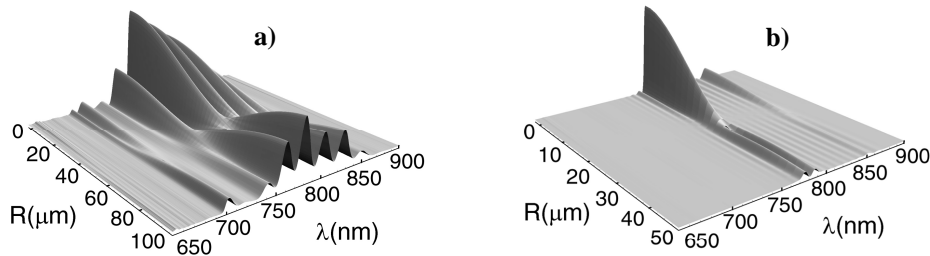


Fig. 3. Variation in the power spectrum with the radial coordinate at the axial positions: a) $z = 2.4$ m ($m = 1$) and b) $z = 0.87$ m ($n = 11$).

Finally, we compare the off-axis dependence for the monochromatic output diffracted field derived from Eq. (2) with that one reported in Eq. (4) of Ref. [9]. From the simulations we realize that the diffracted field assessed by the use of the above-mentioned expressions differs significantly in the non-paraxial regime. In that case, Eq. (2) gives more accurate results. In order to compare both expressions, the irradiance in the transverse plane corresponding to the focal position $z_{57} = 0.17$ m of a two-zone ($N = 2$) DOE with identical period and opening ratio to those used before is plotted in Fig. 4. The solid line was obtained numerically from Eq. (1), whereas the box and the circle symbols denote points assessed by Eq. (4) of Ref. [9], and by Eq. (2) of our manuscript, respectively. After a visual inspection of Fig. 4, it is clear that the best fitting to the expected irradiance values is achieved by means of Eq. (2).

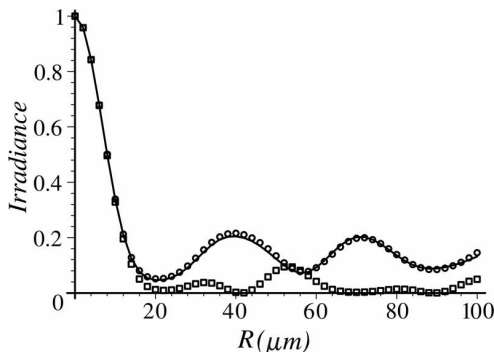


Fig. 4. Normalized irradiance at the focal plane $z_{57} = 0.17$ m, plotted by Eq. (2) (circle symbols), by Eq. (4) of Ref. [9] (box symbols) and by Eq. (1) (solid line) for a DOE with $N = 2$ and $\varepsilon = 4$.

5. Conclusions

A novel analytical solution within the Rayleigh-Sommerfeld theory of diffraction for the off-axis diffracted field caused by the pass of a monochromatic plane wave through a binary DOE with circular symmetry is achieved. The above result allowed us to study the spectral changes in the spectrum of a broadband source diffracted by a periodic, equal-area DOE. The possibility of manipulating the output spectrum of an ultrashort pulse by means of a suitable DOE design finds application, among other fields, in material processing, ultrafast spectroscopy and/or photochemistry.

Acknowledgements

This work was supported by the Direcció General de Investigació Científica y Tècnica, by the Conselleria de Empresa, Universitat i Ciència, Generalitat Valenciana, Spain, and FEDER under the projects FIS2007-62217 and GV/2007/128. Also the project *Science and Applications of Ultrafast and Ultraintense Laser* (SAUUL), within the Consolider program, project CSD2007-013, is acknowledged for its financial support. O. Mendoza-Yero thanks a grant from the “Convenio UJI-Fundació Caixa Castelló (Bancaix)”, grant 06I466.01. Most of the laboratory equipment used in the experiment is located at “Servei Central d’Instrumentació Científica (SCIC)” of the Universitat Jaume I.